Journal of Cluster Science (2022) 33:1751–1762
https://doi.org/10.1007/s10876-021-02101-9

ORIGINAL PAPER

Co-Loading of Cisplatin and Methotrexate in Nanoparticle-Based PCL-PEG System Enhances Lung Cancer Chemotherapy Effects

Elahe Akbari[1,6] · Hanieh Mousazadeh[1] · Younes Hanifehpour[2] · Ebrahim Mostafavi[3] · Armita Mahdavi Gorabi[10] · Kazem Nejati[8] · Peyman keyhanvar[4] · Hamidreza Pazoki-Toroudi[9] · Majid Mohammadhosseini[7] · Abolfazl Akbarzadeh[4,5]

Received: 5 January 2021 / Accepted: 22 May 2021 / Published online: 3 June 2021

Abstract

Since the anticancer drugs exhibited a variety of inhibitory mechanisms in cancer cells, the use of two or more anticancer drugs may have excellent therapeutic effects, particularly in drug-resistant tumors. In this study, the efficient entrapment of two clinically used single-agent drugs, Cisplatin (CDDP) and Methotrexate (MTX) is reported against lung cancer cell lines. Biodegradable polymeric nanoparticles perform to be a favorable environment-responsive controlled drug release system. MTX@CDDP were simultaneously encapsulated into the biodegradable poly (ε-caprolactone) (PCL) modified poly (ethylene glycol) (PEG) copolymer. The spherical nanoparticle was identified via scanning electron microscopy (SEM). Additionally, the antitumor activity and apoptosis induction of designed duel drug-loaded vectors were assessed against A549 cell lines by qRT-PCR, MTT assay, and DAPI staining. The nanoformulation loaded with MTX@CDDP statistically reduced the cell activity of A549. The results indicate that MTX@CDDP-loaded PCL-PEG nanoparticles can be further utilized for treating non-small-cell lung cancer as a promising therapeutic approach.

Graphical Abstract

✉ Abolfazl Akbarzadeh
dr.akbarzadeh2010@gmail.com

[1] Department of Medical Biotechnology, Faculty of Advanced Medical Science, Tabriz University of Medical Science, Tabriz, Iran

[2] Department of Chemistry, Sayyed Jamaleddin Asadabadi University, Asadabad, Iran

[3] Department of Chemical Engineering, Northeastern University, Boston, MA 02115, USA

[4] Stem Cell Research Center, Tabriz University of Medical Sciences, Tabriz, Iran

[5] Universal Scientific Education and Research Network (USERN), Tabriz, Iran

[6] Higher Education Institute of Rab-Rashid, Tabriz, Iran

[7] Department of Chemistry, Shahrood Branch, Islamic Azad University, Shahrood, Iran

[8] Pharmaceutical Sciences Research Center, Ardabil University of Medical Sciences, Ardabil, Iran

[9] Physiology Research Center and Department of Physiology, Faculty of Medicine, Iran University of Medical Sciences, Tehran, Iran

[10] Chronic Diseases Research Center, Endocrinology and Metabolism Population Sciences Institute, Tehran University of Medical Sciences, Tehran, Iran

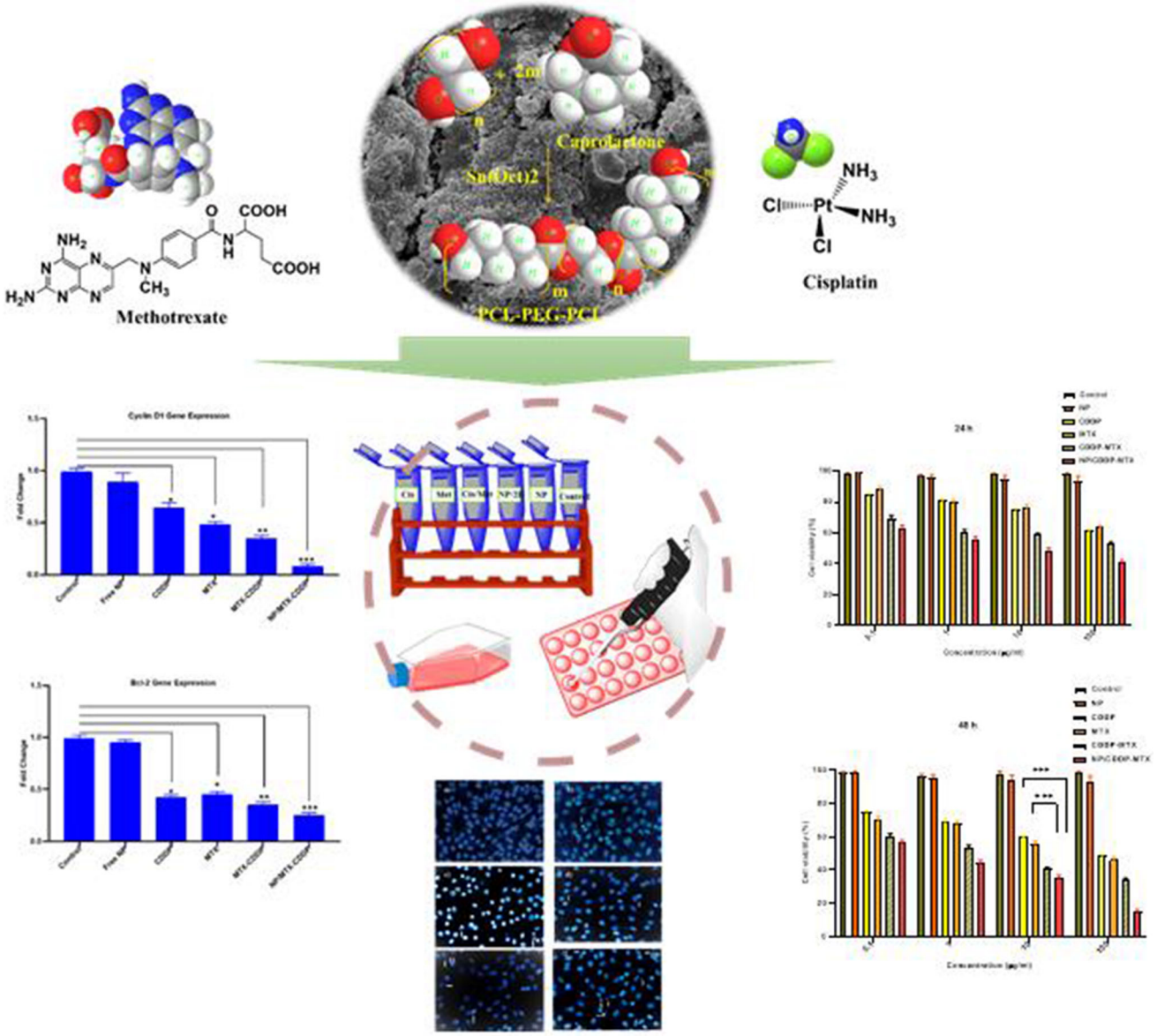

Keywords Cisplatin (CDDP) · Methotrexate (MTX) · Poly(ε-caprolactone) (PCL) · Nanoparticles · Lung cancer

Introduction

The deadliest cancer in the world is Lung cancer [1]. The extension of lung cancer is remarkably related to the changes of unexpected lifestyle, contamination of the environment, and smoking [2, 3]. Lung cancer therapy is usually directed step by step, although coexisting medical conditions and complete health are necessary. Chemotherapy is promising at the greatest phases of the disease, although this method of treatment and radiation therapy are therapeutics in only a portion of all patients suffer from lung cancer. The resistance apparatuses against chemotherapeutic materials lead to chemotherapy failure in lung cancer treatment and deficiency of appropriate curative response [4, 5]. Resistance processes occurred through the P-glycoprotein (P-gp) efflux pumps, which are expressed in human cells and considered in the role of a movement mechanism to transfer drugs away from the cell [5–7]. Hence, the efflux process displays high clinical significance on lung cancer therapy, and numerous P-gp

inhibitor agents have been investigated to control chemotherapy resistance to afford a further prominent result to chemotherapeutic agents [8]. Commonly, lung cancer chemotherapy is followed by using drugs of CDDP and Gentamicin, Paclitaxel, Docetaxel, etc. [9].

As a chemotherapeutic agent, platinum is extensively employed for treating solid tumors [10–12]. Cis-diamminedichloroplatinum (CDDP), is the first FDA-approved platinum compound for the treatment of cancer [13]. It is important to mention that the hydrolyze of CDDP inside the cell leads to greatly sensitive fragments such as $[Pt(NH_3)_2Cl(OH_2)]^+$ and produces intrastrand adducts of 1,2-GpG within the DNA. This adducts disrupts DNA replication and leads to cancer cell death [14, 15]. However, platinum drugs have some natural and main side effects, which may affect the resistance of drugs [16]. The CDDP with higher doses can reduce tumor resistance but do not involve target-specific delivery [17].

Thus, the targeted distribution process can remarkably decrease the side effects of CDDP and increase its efficacy. Methotrexate (MTX) is an anionic anticancer drug accompanied with a chemotherapeutic folic acid structure popular for its effectiveness in various cancer therapy such as breast, leukemia, lymphoma, neck and head, lung cancer, and osteosarcoma [18, 19]. MTX interrupts cellular folate metabolism by preventing its target enzyme, dihydrofolate reductase (DHFR). MTX inhibits (DHFR) activity and so leads to suppression of the synthesis of RNA, DNA, and cell proliferation [20].

The co-administration and co-localization of the two drugs in a vector have revealed respectable synergistic properties on cancer therapy [21]. As proposed, MTX can prevent the platinum–DNA adduct repair and increase the apoptosis process of CDDP-resistant tumor cells by enhancing the expression level of proapoptotic proteins. However, the low biological half-life and great flow degree of MTX in comparison to the penetration degree wants a high direction dose for controlling the resistance of drug [22], and lead to several obstacles on its clinical applications. Thus, the appropriate chemotherapeutic drugs with optimal dosage formulations lead to an improved therapeutic index with the least side effects.

The development of a synergic feature in the production of appropriate multi-drug delivery systems (MDDS) more effectively improved some malignancies treatment [23]. In 1987, Stouter G et al.; reported combination chemotherapy of CDDP and MTX as the main active factor in the treatment of advanced transitional cell cancer of the urothelial region [24]. Corral DA and collages reported the combination chemotherapy using MTX, CDDP, and bleomycin in patients considering developed genitourinary squamous cell carcinoma [25]. The investigation of results demonstrated that an elevated but short-lived overall response rate and a down total response rate with controllable toxicity. Hecheng Ma et al.; developed a novel route for the osteosarcoma treatment by employing poly (lactic-co-glycolic acid)- poly (ethylene glycol) poly(lactic-co-glycolic acid) (PLGA-PEG-PLGA) hydrogel-based thermosensitive system for co-delivery of various drugs, consisting of CDDP, MTX, and doxorubicin (DOX). These encapsulated vectors improved effectiveness in the prevention of tumor growth and improved regulation of the apoptosis-related gene expressions, compared to the encapsulated vectors with DOX-CDDP or DOX [26].

However, to the best of our knowledge, no further paper was reported for localized co-delivery of CDDP, MTX-based biodegradable poly(ε-caprolactone) (PCL) modified poly (ethylene glycol) (PEG) in lung cancer therapy.

Poly(caprolactone) (PCL) is a biodegradable semi-crystalline poly(α-hydroxy ester), generally considered a nontoxic, tissue-compatible polymer [27, 28]. However, the rate of degradation of PCL is relatively slow due to its high crystallinity and hydrophobic nature. (PEG) is known as a hydrophilic biocompatible polymer with significant biological or pharmaceutical applications. However, PEGylated therapeutics critically leads to high aqueous solubility and in vivo circulation time with low enzymatic degradation. In addition, the PEGylation process leads to passive tumor targeting with modified permeability and retention (EPR) results [29]. Several restrictions of the conventional DDS like lack of targeting capacity multi-drug resistance and poor water solubility can be improved by the nanoformulations of DDS [30, 31]. Hence, the designed nanocarriers can circumvent restrictions produced by both CDDP and MTX, and thus provide the protection of drugs against degradation, enhance the bioavailability, and decrease probable side effects. Notably, the nanocarriers can achieve target tissues, definite specious tissues, and tumors because of their excellent properties such as Brownian movement, small particle size, surface functionality, and large surface area [32–36]

Herein, the co-administration and co-localization of CDDP and MTX into PCL-PEG nanoplatform investigated and in vitro examination were followed to assess the synergistic cytotoxic effects of co-loaded PCL-PEG nanoparticles towards A549 lung cancer cell. As a novel therapeutic strategy, the co-loaded nanocapsules approaches can be further utilized for treating non-small-cell lung cancer to hold the possibility for succeeding therapeutic effects with decreasing adverse effects of the drug.

Experimental

Materials and Methods

ε-Caprolactone $(PCL)_{1000}$, polyethylene glycol $(PEG)_{4000}$, stannous octoate $(Sn(Oct)_2$, and polyvinyl alcohol (PVA): were obtained from Sigma-Aldrich (USA). MTX and CDDP were purchased from medical science pharmaceuticals, Tabriz, Iran. Human lung cancer cell line A549 was obtained from the Pasteur Institute of Iran. RPMI-1640 medium, fetal bovine serum (FBS), MTT (3(4, 5-dimethyl thiazol-2-yl) 2, 5-diphenyl-tetrazolium bromide), streptomycin and penicillin G and Dimethyl sulfoxide (DMSO) were purchased from Sigma-Aldrich. Biotrade kit for extraction RNA, cDNA synthesizes kit, and QuantiTect SYBR Green Real-time PCR (RT-PCR) Kit was purchased from Takara. 4',6-diamidino-2-phenylindole (DAPI). The chemical structures of the copolymer were characterized by Fourier transform infrared spectroscopy (FTIR). The hydrodynamic diameter of the obtained co-loaded NPs was evaluated by measuring the dynamic light scattering (Malvern Instruments Ltd., Malvern, UK). The surface morphology of co-loaded NPs was examined by using a scanning electron microscope (VEGA/TESCAN). The cell toxicity was evaluated by MTT assay. For DAPI, a fluorescence microscope (Olympus microscope Bh2-RFCA, Japan) was employed.

Synthesis of PCL-PEG Copolymers

The copolymer was acquired through the ring-opening polymerization ε-caprolactone. First, the reaction was followed with ethylene glycol (3gr) as initiator and ε-caprolactone (7.4 gr) in a dry three-necked flask under nitrogen atmosphere at 130 °C to complete melting. Then, the polymerization was completed in the presence of $Sn(Oct)_2$ (0.05% (w/w) at 180 °C for 6 h [37]. Next, the generated product was dissolved in dichloromethane, and finally, the precipitation process followed in cold diethyl ether solvent.

CDDP and MTX-Loaded PCL-PEG Nanoparticles

First, CDDP (0.3 mg) and MTX (0.3 mg) were dissolved in 1 mL methanol, and the obtained solution was added into PCL-PEG (20 mg) in 3 ml dichloromethane. Then, polyvinyl alcohol (PVA) was added to this solution and the whole solution was exposed to ultrasound irradiation for 2 min. The obtained solution is centrifuged at 9000 rpm for 25 min. The supernatant was isolated and used to compare with the total amount of CDDP and MTX to determine the CDDP and MTX in the encapsulation efficiency of the nanoparticles. The amount of unencapsulated CDDP, MTX in the supernatant was measured using an ultraviolet 2550 spectrophotometer (Shimadzu).

Cell Culture

Cultured in RPMI, cell line A549 was supplemented with 1% penicillin–streptomycin and 10% FBS at 37 °C in a moistened atmosphere containing 5% CO_2. About 5×10^3 cells were seeded in each well of 96-well plates.

Cytotoxicity Assays

Using MTT assay, the A549 cancer cell line was reported as the target cell line and utilized for the cytotoxicity assessment of the nanocarriers. The antitumor activity of the CDDP@MTX loaded PCL-PEG nanoparticles was evaluated by the MTT process according to the previous description [38]. First, 5×10^3 cells per well were seed in a 96-well microplate (Coaster from Corning, NY) and incubated at 37 °C for 24 h. Then, the various doses of free MTX, CDDP, and CDDP@MTX loaded PCL-PEG-PCL (0.1 to 100 μg/mL) were incubated for 24, 48, and 72 h. The appropriate concentration of MTT solution at the range of 0.5 mg/mL in each 150 μL of media was added well. The incubation of microplates was followed at 37 °C in a wet atmosphere containing 5% CO_2 and 95% air for 4 h. Finally, the content in the wells was detached and 200 μL pure DMSO was added to each well of the microplate. The ELISA plate reader at 570 nm was used for the determination of absorbance considering a wavelength of 630 nm as a reference.

Also, Compusyn software version 1.0 (ComboSyn, Inc.) was used to determine the nature of the interaction between CDDP and MTX in MTX@CDDP NPs after 48 h treatment.

cDNA Synthesis, Final RNA Extraction, and Real-time PCR

The extraction of total RNA was followed on the treated cells with MTX@CDDP loaded PCL-PEG-PCL nanoparticles after 48 h treatments. The density of RNA was determined by nanodrop. The RNA samples were converted to cDNA by using the strand cDNA synthesis kit. For each sample of reaction, 1 μg/μL of total RNA was used. Also, 10 μL of nuclease-free water, 1 μL of oligo dT primer, 4 μL of 5X Reaction Buffer, 1 μL of RevertAid M-MuLV Reverse Transcriptase,1 μL RiboLock RNase inhibitor and 2 μL of dNTP Mix and were put into each as-prepared sample reaction. Then, the blend of reactions was incubated in the following settings: 37 °C, Reverse Transcription for 15 min and 85 °C, 5 s inactivation of reverse transcriptase with heat treatment; 4 °C. To determine

cyclin D1 and Bcl2 expression levels, Real-time PCR was used. For Real-time PCR reaction, 5 µl of Real-time PCR master mix, 0.5 µl (1 µl) of forward and reverse primers of cyclin D1, Bcl2 and 2 µL of cDNA sample, and 2 µL of deionized water were used. *GAPDH gene* was *used* as an internal control. All primer sequences are provided in Table 1. Based on the following conditions, the incubation of reaction mixture was carried out: 5 min, 95 °C, (Holding step) 1 cycle; 95 °C, 15 s, (Denaturation) 40 cycles; 60 °C, 15 s, (Annealing) 40 cycles; 72 °C, 30 s, (Extension) 40 cycles; 72–95 °C, 1 cycle (Melting).

DAPI Staining

In this study, the DAPI staining process was followed for apoptosis induction. This process evaluated the fragmented and condensed nuclei of the cells created by apoptosis. Briefly, A549 cells were seeded on six-well plates (5×10^4 cells per well), and incubation after 24 h at 37 °C, they treated with free CDDP and MTX, as well as MTX@CDDP loaded PCL-PEG-PCL nanoparticles. Later 48 h, the cells were washed with fresh PBS and then settled with 4% (v/v) formaldehyde at room temperature for 15 min. Afterward, the cells were permeabilized with Triton X100 (0.1% w/v) for 5 min after three times washing with PBS. The cells were washed again with PBS and stained with 300 ng/mL DAPI for 15 min. Finally, the cells using fluorescence microscope (Olympus microscope Bh2-RFCA, Japan) were imaged.

Statistical Analysis

The results as mean ± SD from at least three individualistic tests are reported. The ANOVA test was completed for statistical analysis, and examining consequence with a p-value is < 0.05.

Results and Discussion

In cancer therapy, most proposed formulations present certain drawbacks related to low drug loading, toxicity, and/or an unsuitable release pattern [39]. An ideal formulation should supply biocompatible nanosized particles and high drug loading with sustained-release characteristics, allowing drug release in the target site at a therapeutic concentration, thereby minimizing drug inefficiency and adverse effects. Various approaches have been investigated in this line [40, 41]. Drug delivery based on nanotechnology is estimated to intensely improve combination cancer therapy via the monitoring of the accumulation and distribution of multiple drug forms [42]. In this work, co-administration and co-localization of CDDP and MTX were formulated into PCL-PEG nanoplatform. Considerably, this biodegradable nanocarrier decreased unwanted uptake or interactions into normal sites, where the structure of the copolymer controls the amount and site of drug release. The double emulsion (w/o/w) technique was used to prepare nanoparticles (Scheme 1). The efficient factors on entrapment efficiency using this procedure including of the volume of the outer aqueous phase, the volume of the inner aqueous phase, copolymer concentration in organic solution, the first homogenized time and speed, and the second homogenized time and speed.

Measurement and Characterization of Nanoparticles

The FTIR spectra of PCL-PEG copolymer and CDDP@MTX co-loaded PCL-PEG copolymer are seen in Fig. 1. The absorption bands at 1730 cm^{-1} correspond to C = O carbonyl ester groups, bands at 2938 and 2869 cm^{-1} and 1102–1239 cm^{-1} were attributed to –CH group from an aliphatic chain and stretching bands C-O, respectively. The typical bands at 1645 cm^{-1}, and 1523, 1460 cm^{-1} attributed to C = O carbonyl and C = C stretching of the aromatic ring of MTX. The peaks at 3442 and 738 cm^{-1} corresponding to the N–H stretching and bending vibrations of CDDP, respectively.

The morphological characterization of MTX@CDDP NPs was investigated by SEM. The images of the drug-loaded NPs shown their regular spherical shape. The surface morphology of NPs was smooth with a regular spherical shape. The size distribution of NPs was narrow with a mean particle diameter of ∼ 100 nm. (Fig. 2a, b).

Table 1 Sequences of primers for real-time PCR

Primers name	Sequence (5' to 3')	PCR product size
R Bcl2	CCTGTGGATGACTGAGTACC	128 bp
F Bcl2	GAGACAGCCAGGAGA AATCA	
R cyclin D1	TCTGGAGAGGAAGCGTGTGA	148 bp
F cyclin D1	TGCCCTCTGTGCCACAGATG	
R GAPDH	GGCATGGACTGTGGTCATCA	142 bp
F GAPDH	GGCATGGACTGTGGTCATCA	

Scheme 1 Preparation of PCL - PEG -PCL triblock copolymers

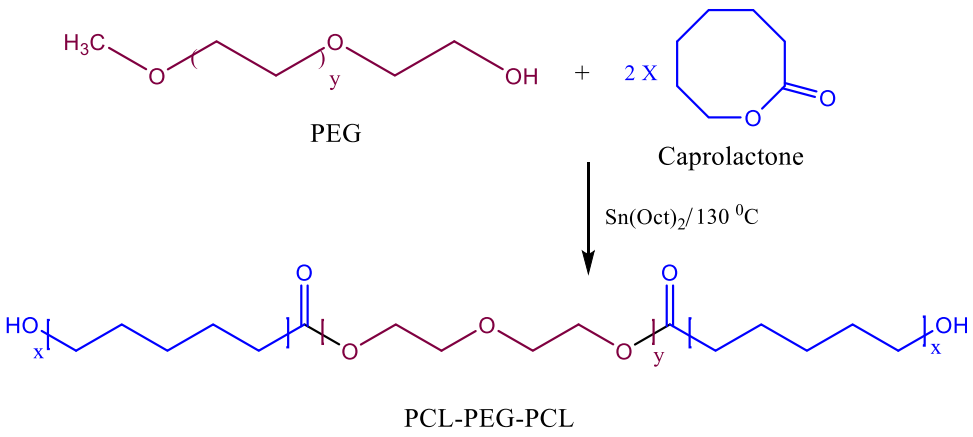

Fig. 1 **a** FTIR spectra of PCL-PEG copolymer and **b** MTX@CDDP loaded PCL-PEG NPs

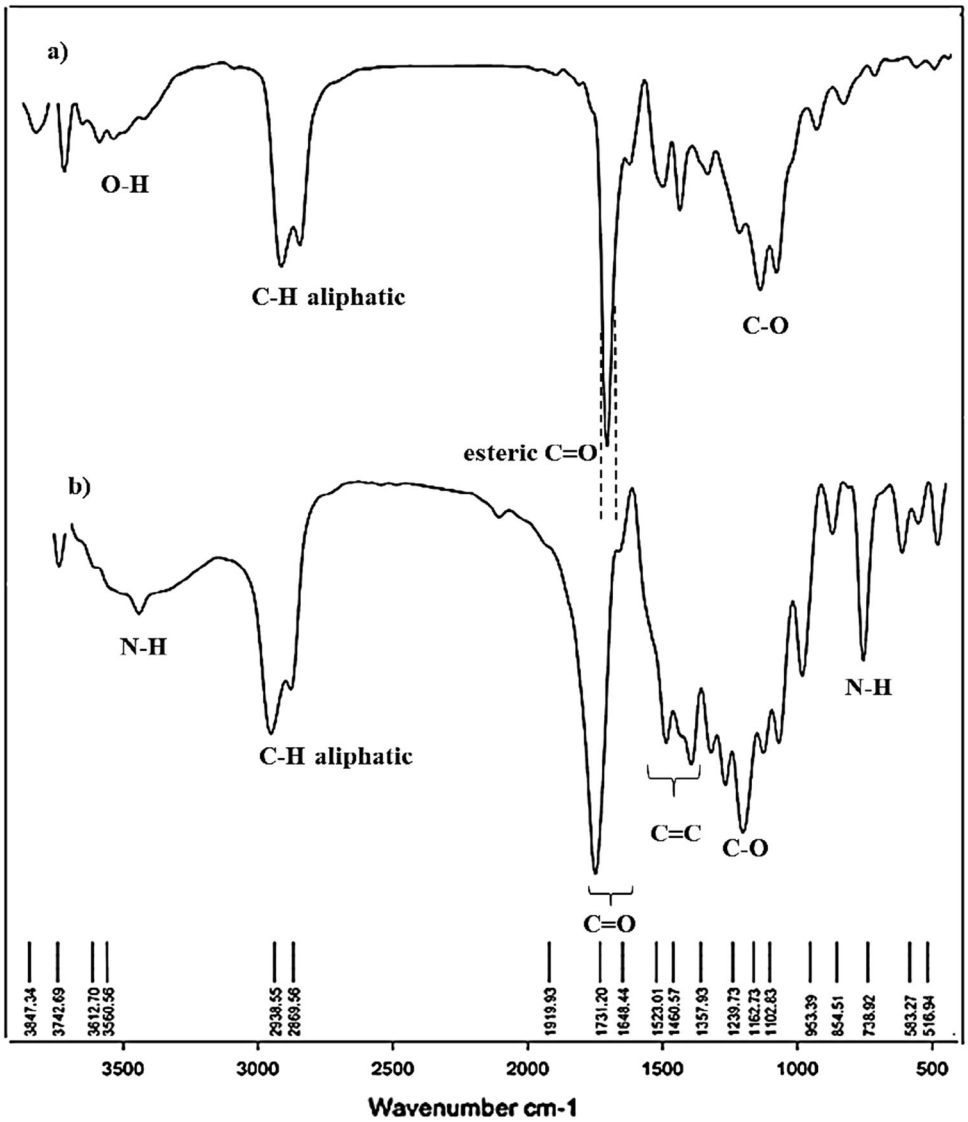

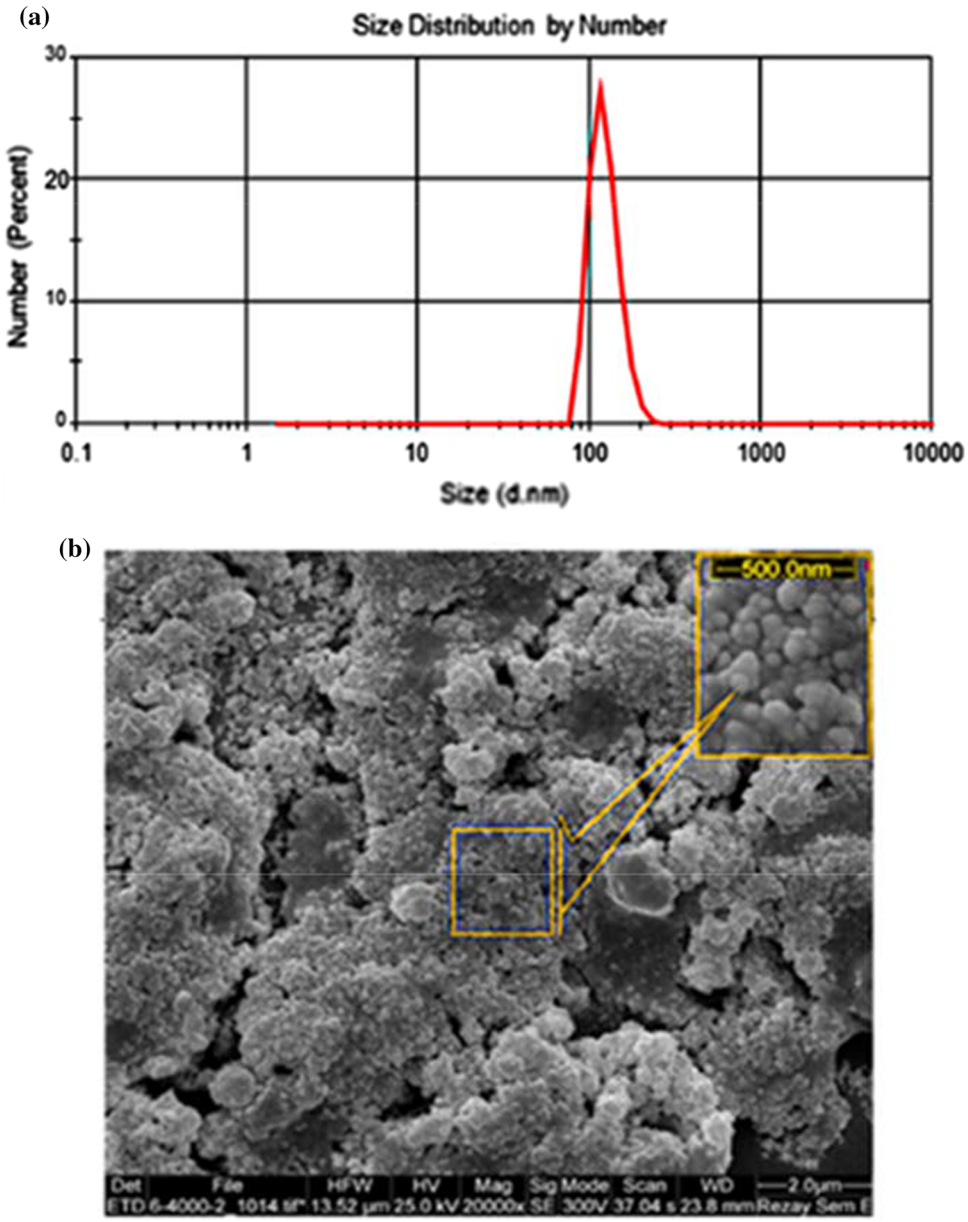

Fig. 2 Dynamic light scattering (DLS) histogram and the scanning electron microscopy (SEM) micrograph of MTX@CDDP loaded PCL-PEG NPs

In Vitro Cell Cytotoxicity (MTT Assay)

The cytotoxicity of the MTX@CDDP co-loaded PCL-PEG nanoparticles was analyzed via MTT analyses for 24, 48 h (Fig. 3a). Various concentrations of (0.1, 1, 10, and 100 μg/mL) MTX@ CDDP co-loaded PCL-PEG nanoparticles were selected for the cytotoxicity measurement. The cytotoxicity of MTX@ CDDP dual anticancer drugs in free form or co-loaded PCL-PEG nanoparticles were enhanced in a dose-dependent fashion. The biocompatibility of the free polymer was demonstrated well in the MTT graph as it shows less than 10% inhibition in all the combinations. The cell viability of MTX@ CDDP co-loaded PCL-PEG nanoparticles was much higher than that of free MTX@CDDP analogs. Most likely, the sustained release of MTX and CDDP from MTX@CDDP loaded PCL-PEG nanoparticles lead to excessive cell death. In contrast, MTX@CDDP NPs had no significant effect on the viability percentage of NIH-3T3 cells after 24, 48, 72 h treatment (Fig. 3b).

CompuSyn software was used to analyze the precise nature of the interaction between CDDP and MTX in the combination treatments through the Median-effect method. The resulting CI theorem of Chou-Talalay offers a quantitative definition for additive effect (CI = 1), synergism (CI < 1), and antagonism (CI > 1) in drug combinations. According to our results, the half-maximum combination index value for MTX@CDDP NPs in A549 cells was

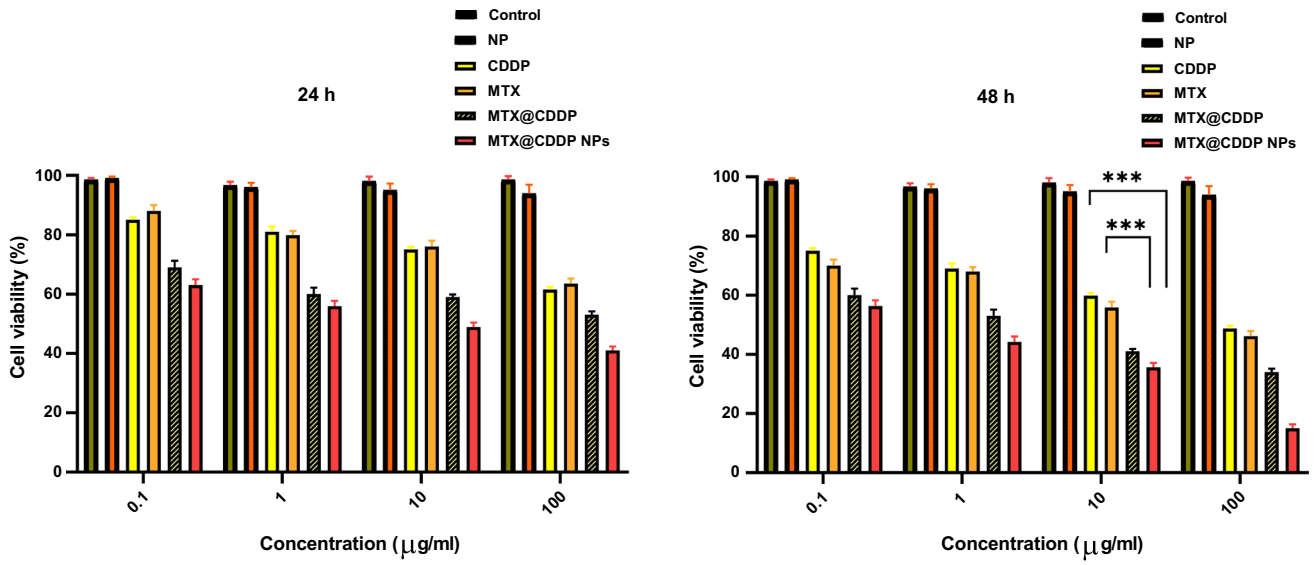

Fig. 3 Cell growth inhibition rates in the presence of various concentrations of MTX, CDDP, MTX@CDDP, and MTX@CDDP loaded PCL-PEG on A549 cell lines after 24, 48 h incubation

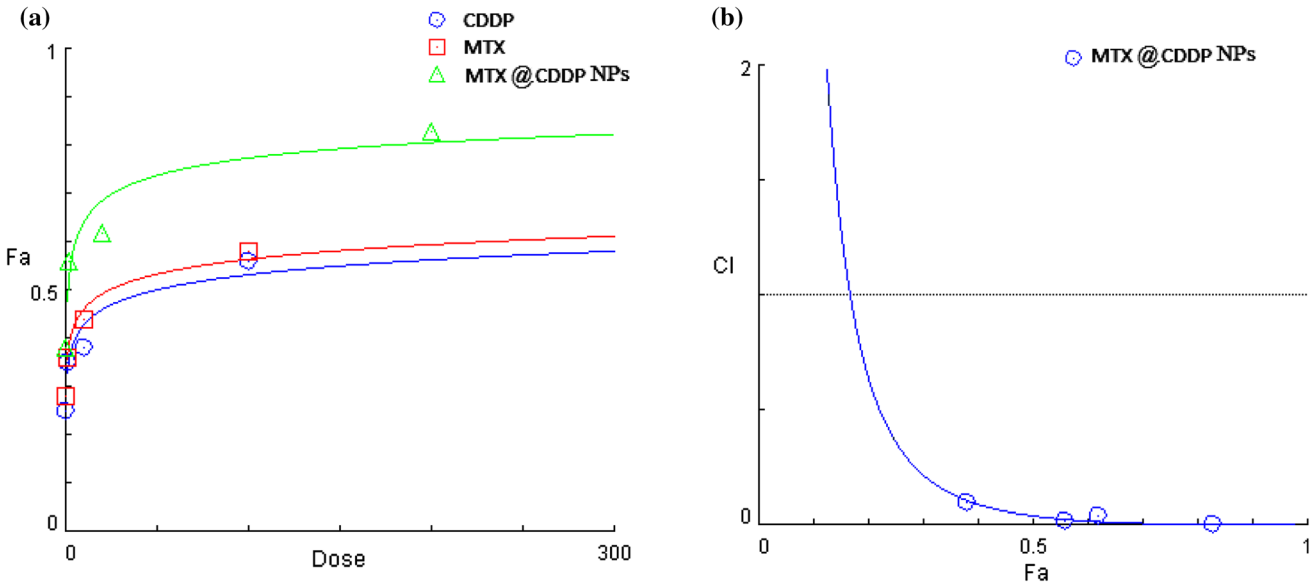

Fig. 4 **a** The dose–effect plot (Fa-Dose plot) and **b** the combination index plot (Fa-CI plot) for the synergistic growth inhibitory effects of MTX@CDDP NPs on A549 cell lines. (Combination index (CI) was calculated by isobologram analysis using the Chou-Talalay method. CI = 1, additive effect; CI < 1, s

calculated 0.004, indicating the strong synergism effect of CDDP and MTX in dual-drug-loaded PCL-PEG NPs. A graphical representation of the obtained results was the dose–effect (Fa-Dose plot) and combination index curves (Fa–CI plot), in which the CI values were plotted against the corresponding effect levels (Fig. 4a, b).

Quantitative Real-Time PCR (qPCR)

The bcl-2 gene is an anti-apoptotic protein with apoptosis-blocking effects [43]. A key cell cycle regulator of the G_1 to S phase progression is cyclin D1 [44]. Thus, it is accounted a therapeutic target to cancer. Besides, cyclin D1 controls senescence, tumorigenesis, and apoptosis for the regulation of cell proliferation. The over-expression of cyclin D1 results in apoptosis resistance in cell lines. Here, the expression of both bcl2 and cyclin D1 was explored for the evaluation of the cytotoxic effects of designed co-loaded nanocarrier on gene expression levels. The levels of Bcl2 gene expression and cyclin D1 were evaluated via Real-Time PCR. Changes in cyclin D1 and Bcl2 expression levels between the treated and control A549 cells were

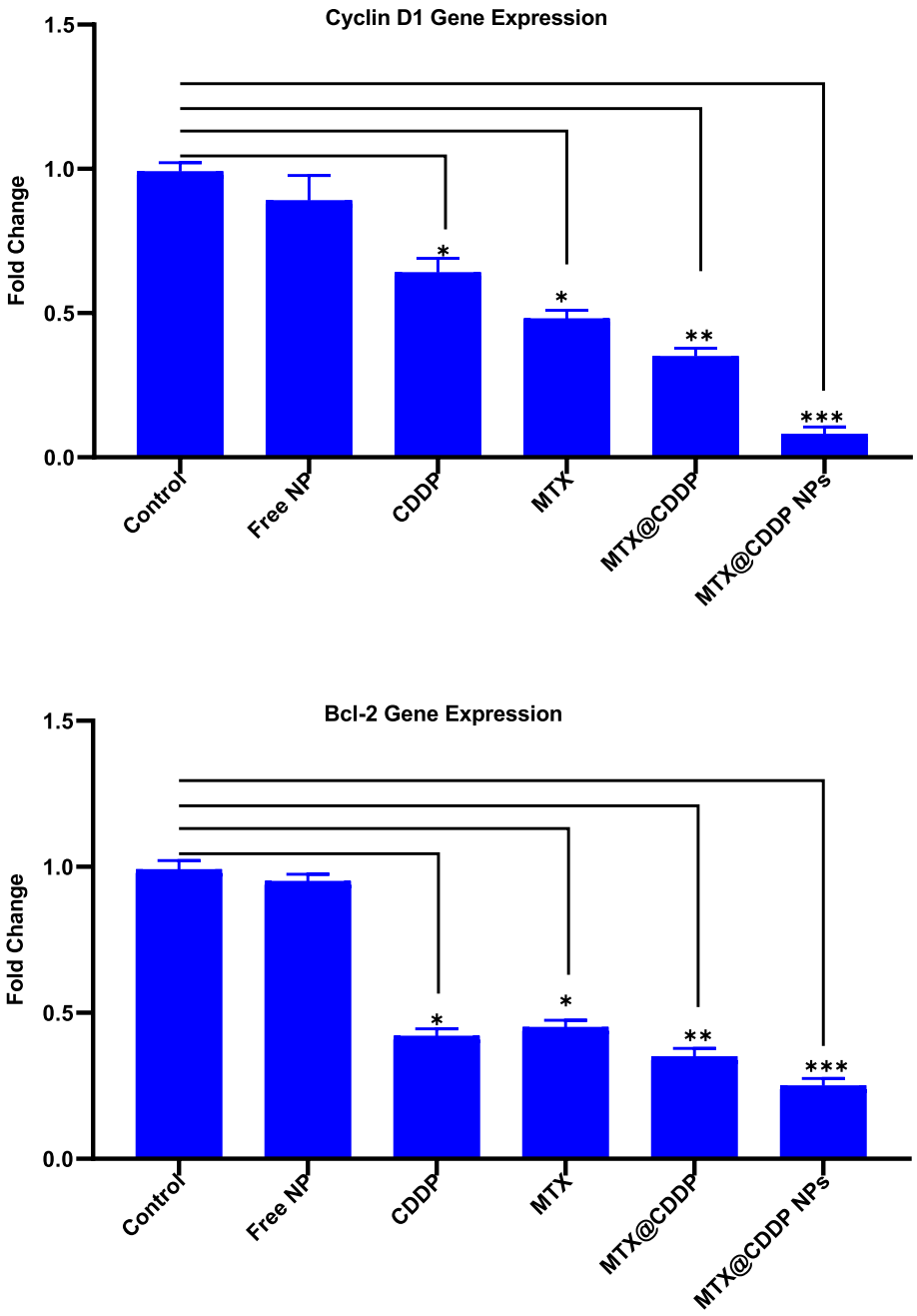

Fig. 5 Real-time PCR results after treatments MTX, CDDP, MTX@CDDP, and MTX@CDDP loaded PCL-PEG about cyclinD1 and bcl2. synergistic effect; CI > 1, antagonistic effect. Data represented are from three independent experiments)

normalized to GAPDH mRNA levels and therefore computed through the 2-Δ ΔCT route. Figure 5 exhibits that the expression level of cyclin D1 significantly decreased in both MTX and CDDP and CDDP@MTX co-loaded PCL-PEG-PCL nanoparticle treated cells. The expression of bcl-2 also decreased similarly by the cells treated MTX and CDDP and MTX@CDDP co-loaded PCL-PEG-PCL nanoparticle with ($p < 0.05$), and ($p < 0.001$).

DAPI Staining Evaluation

In the present study, apoptosis-inducing characteristics of the MTX@CDDP loaded PCL-PEG nanoparticles were compared with the intact free CDDP, free MTX, MTX@CDDP against A549 cells employing DAPI staining analysis. The results demonstrated that the formation of chromatin fragments on the cells treated with free drugs or

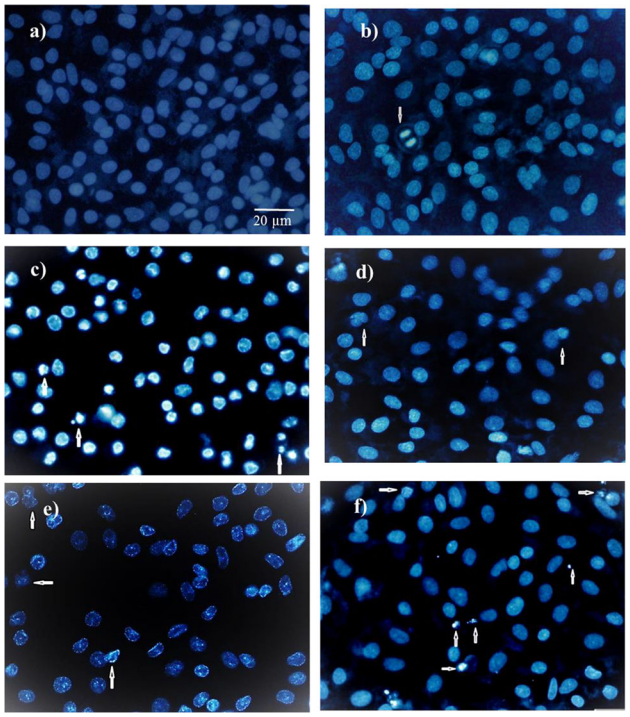

Fig. 6 Fluorescent microscope images of **a** Control, **b** NPs, **c** MTX, **d** CDDP, **e** MTX@CDDP, and **f** MTX@CDDP loaded PCL-PEG on A549 cell lines

MTX@CDDP loaded PCL-PEG nanoparticles compared with the untreated cells Fig. 6. In addition, the frequentness of chromatin fragmentation in MTX@CDDP loaded PCL-PEG treated cells was higher than free drugs, which revealed that the produced duel drug carrier is an exceptional selection for an efficient drug delivery process.

Conclusions

In summary, MTX and/or CDDP encapsulated PCL-EG nanoparticles were effectively prepared through the formation of interfacial polymer deposition. Spherical nanoparticles with elevated drug-loading effectiveness were achieved. FTIR spectra exhibited no changes after the nanoencapsulation process. Besides, CDDP@MTX nanoparticles exhibited a statistically important reduction of A549 cell viability through MTT assays due to their induced synergistic effects. The apoptosis-inducing properties of the duel drug-loaded nanoparticles were followed by using DAPI analysis. The treated cells with these nanoencapsulation lead to the high intensity of chromatin fragmentation compared to the free drugs. In addition, the expression levels of both bcl2 and cyclin D1 have considerably reduced in both MTX and CDDP and MTX@CDDP co-loaded PCL-PEG-PCL nanoparticle treated cells. These results provide a clear description of biodegradable nanoparticles for the development of efficient carriers for drug delivery. Further, it establishes the use of two or more anticancer drugs can enhance therapeutic effects, particularly in drug-resistant tumors.

Acknowledgements Research reported in this publication was supported by Elite Researcher Grant Committee under award number [971185] from the National Institutes for Medical Research Development (NIMAD), Tehran, Iran.

Declarations

Conflict of interest The authors declare that they have no competing interests. The authors alone are responsible for the content and writing of this article.

References

1. A. Anwar and N. Waheed (2015). Galactosemia: clinical manifestations, diagnosis and outcome of early management. *Ann Pak Inst Med Sci.* **11** (4), 190–194.
2. A. Waheed, A. Gupta, and P. Patel (2015). Targeted drug delivery systems for lung cancer. *PharmaTutor.* **3** (2), 38–42.
3. L. Chen, A. Nan, N. Zhang, Y. Jia, X. Li, Y. Ling, et al. (2019). Circular RNA 100146 functions as an oncogene through direct binding to miR-361-3p and miR-615-5p in non-small cell lung cancer. *Molecular cancer.* **18** (1), 1–8.
4. P. C. Huber, C. H. Maruiama, and W. P. Almeida (2010). Glicoproteína-P, resistência a múltiplas drogas (MDR) e relação estrutura-atividade de moduladores. *Química Nova.* **33** (10), 2148–2154.
5. S. Niu, G. R. Williams, J. Wu, J. Wu, X. Zhang, H. Zheng, et al. (2019). A novel chitosan-based nanomedicine for multi-drug resistant breast cancer therapy. *Chemical Engineering Journal.* **369**, 134–149.
6. Ke. Xj, Y. F. Cheng, N. Yu, and Q. Di (2019). Effects of carbamazepine on the P-gp and CYP3A expression correlated with PXR or NF-κB activity in the bEnd 3 cells. *Neuroscience letters.* **690**, 48–55.
7. J. M. Albano, L. N. de Morais Ribeiro, V. M. Couto, M. B. Messias, G. H. R. da Silva, M. C. Breitkreitz, et al. (2019). Rational design of polymer-lipid nanoparticles for docetaxel delivery. *Colloids and Surfaces B: Biointerfaces.* **175**, 56–64.
8. W. Chearwae, S. Anuchapreeda, K. Nandigama, S. Ambudkar, and P. Limtrakul (2004). Biochemical mechanism of modulation of human P-glycoprotein (ABCB1) by curcumin I, II, and III purified from Turmeric powder. *Biochemical Pharmacology.* **68** (10), 2043–2052.
9. P. Zarogoulidis, D. Petridis, C. Ritzoulis, K. Darwiche, D. Spyratos, H. Huang, et al. (2013). Establishing the optimal nebulization system for paclitaxel, docetaxel, cisplatin, carboplatin and gemcitabine: back to drawing the residual cup. *International Journal of Pharmaceutics.* **453** (2), 480–487.
10. H. Xiao, R. Qi, T. Li, S. G. Awuah, Y. Zheng, W. Wei, et al. (2017). Maximizing synergistic activity when combining RNAi and platinum-based anticancer agents. *Journal of the American Chemical Society.* **139** (8), 3033–3044.
11. J. Shen, Y. Zhu, H. Shi, and Y. Liu (2018). Multifunctional nanodrug delivery systems for platinum-based anticancer drugs. *Progress in Chemistry.* **30** (10), 1557–1572.
12. K. Nejati-Koshki, A. Akbarzadeh, and M. Pourhassan-Moghaddam (2014). Curcumin inhibits leptin gene expression and

secretion in breast cancer cells by estrogen receptors. *Cancer Cell International.* **14** (1), 1–7.
13. R. B. Weiss and M. C. Christian (1993). New cisplatin analogues in development. *Drugs.* **46** (3), 360–377.
14. Jamieson E. Lippard (1999). *SJ Chem. Rev.* **99**, 2467.
15. T. Boulikas, A. Pantos, E. Bellis, and P. Christofis (2007). Designing platinum compounds in cancer: structures and mechanisms. *Cancer Ther.* **5**, 537–583.
16. R. Sharma, P. Tobin, and S. J. Clarke (2005). Management of chemotherapy-induced nausea, vomiting, oral mucositis, and diarrhoea. *The lancet oncology.* **6** (2), 93–102.
17. S. M. Sancho-Martínez, L. Prieto-García, M. Prieto, J. M. Lopez-Novoa, and F. J. López-Hernández (2012). Subcellular targets of cisplatin cytotoxicity: an integrated view. *Pharmacology amd Therapeutics.* **136** (1), 35–55.
18. A. Kim, J.-E. Lee, W.-S. Jang, S.-J. Lee, S. Park, H. J. Kang, et al. (2012). A combination of methotrexate and irradiation promotes cell death in NK/T-cell lymphoma cells via down-regulation of NF-κB signaling. *Leukemia research.* **36** (3), 350–357.
19. Z. Pan, G. Yang, H. He, G. Zhao, T. Yuan, Y. Li, et al. (2016). Concurrent radiotherapy and intrathecal methotrexate for treating leptomeningeal metastasis from solid tumors with adverse prognostic factors: a prospective and single-arm study. *International Journal of Cancer.* **139** (8), 1864–1872.
20. I. D. Goldman and L. H. Matherly (1985). The cellular pharmacology of methotrexate. *Pharmacology & Therapeutics.* **28** (1), 77–102.
21. P. Parashar, C. B. Tripathi, M. Arya, J. Kanoujia, M. Singh, A. Yadav, et al. (2019). A synergistic approach for management of lung carcinoma through folic acid functionalized co-therapy of capsaicin and gefitinib nanoparticles: enhanced apoptosis and metalloproteinase-9 down-regulation. *Phytomedicine.* **53**, 107–123.
22. Y. Pan, N. G. Sahoo, and L. Li (2012). The application of graphene oxide in drug delivery. *Expert Opinion on Drug Delivery.* **9** (11), 1365–1376.
23. I. Brigger, C. Dubernet, and P. Couvreur (2012). Nanoparticles in cancer therapy and diagnosis. *Advanced Drug Delivery Reviews.* **64**, 24–36.
24. G. Stoter, T. Splinter, J. Child, S. Fosså, L. Denis, A. Van Oosterom, et al. (1987). Combination chemotherapy with cisplatin and methotrexate in advanced transitional cell cancer of the bladder. *The Journal of Urology.* **137** (4), 663–667.
25. D. A. Corral, A. Sella, C. A. Pettaway, R. J. Amato, D. M. Jones, and J. Ellerhorst (1998). Combination chemotherapy for metastatic or locally advanced genitourinary squamous cell carcinoma: a phase II study of methotrexate, cisplatin and bleomycin. *The Journal of Urology.* **160** (5), 1770–1774.
26. H. Ma, C. He, Y. Cheng, Z. Yang, J. Zang, J. Liu, et al. (2015). Localized co-delivery of doxorubicin, cisplatin, and methotrexate by thermosensitive hydrogels for enhanced osteosarcoma treatment. *ACS Applied Materials & Interfaces.* **7** (49), 27040–27048.
27. M. Avella, F. Bondioli, V. Cannillo, E. Di Pace, M. E. Errico, A. M. Ferrari, et al. (2006). Poly (ε-caprolactone)-based nanocomposites: Influence of compatibilization on properties of poly (ε-caprolactone)–silica nanocomposites. *Composites Science and Technology.* **66** (7–8), 886–894.
28. N. Asadi, N. Annabi, E. Mostafavi, M. Anzabi, R. Khalilov, S. Saghfi, et al. (2018). Synthesis, characterization and in vitro evaluation of magnetic nanoparticles modified with PCL–PEG–PCL for controlled delivery of 5FU. *Artificial Cells, Nanomedicine, and Biotechnology.* **46** (sup1), 938–945.
29. J. S. Suk, Q. Xu, N. Kim, J. Hanes, and L. M. Ensign (2016). PEGylation as a strategy for improving nanoparticle-based drug and gene delivery. *Advanced Drug Delivery Reviews.* **99**, 28–51.
30. M. Chidambaram, R. Manavalan, and K. Kathiresan (2011). Nanotherapeutics to overcome conventional cancer chemotherapy limitations. *Journal of Pharmacy & Pharmaceutical Sciences.* **14** (1), 67–77.
31. P. Soltantabar, E. L. Calubaquib, E. Mostafavi, M. C. Biewer, and M. C. Stefan (2020). Enhancement of loading efficiency by co-loading of doxorubicin and quercetin in thermoresponsive polymeric micelles. *Biomacromolecules.* **21** (4), 1427–1436.
32. E. Mostafavi, P. Soltantabar, and T. J. Webster (2019). Nanotechnology and picotechnology: A new arena for translational medicine. Biomaterials in Translational Medicine: Elsevier, p. 191–212.
33. E. Mostafavi, D. Medina-Cruz, K. Kalantari, A. Taymoori, P. Soltantabar, and T. J. Webster (2020). Electroconductive nanobiomaterials for tissue engineering and regenerative medicine. *Bioelectricity.* **2** (2), 120–149.
34. P. Parashar, C. B. Tripathi, M. Arya, J. Kanoujia, M. Singh, A. Yadav, et al. (2018). Biotinylated naringenin intensified anticancer effect of gefitinib in urethane-induced lung cancer in rats: favourable modulation of apoptotic regulators and serum metabolomics. *Artificial Cells, Nanomedicine, and Biotechnology.* **46** (sup3), S598–S610.
35. S. Fekri Aval, A. Akbarzadeh, M. R. Yamchi, F. Zarghami, K. Nejati-Koshki, and N. Zarghami (2016). Gene silencing effect of SiRNA-magnetic modified with biodegradable copolymer nanoparticles on hTERT gene expression in lung cancer cell line. *Artificial Cells, Nanomedicine, and Biotechnology.* **44** (1), 188–193.
36. E. Adlravan, K. Nejati, M. A. Karimi, H. Mousazadeh, A. Abbasi, and M. Dadashpour (2021). Potential activity of free and PLGA/PEG nanoencapsulated nasturtium officinale extract in inducing cytotoxicity and apoptosis in human lung carcinoma A549 cells. *Journal of Drug Delivery Science and Technology.* **61**, 102256.
37. J. Yang, S.-B. Park, H.-G. Yoon, Y.-M. Huh, and S. Haam (2006). Preparation of poly ε-caprolactone nanoparticles containing magnetite for magnetic drug carrier. *International Journal of Pharmaceutics.* **324** (2), 185–190.
38. S. Rasouli, S. Davaran, F. Rasouli, M. Mahkam, and R. Salehi (2014). Positively charged functionalized silica nanoparticles as nontoxic carriers for triggered anticancer drug release. *Designed Monomers and Polymers.* **17** (3), 227–237.
39. K. Nejati-Koshki, M. Mesgari, E. Ebrahimi, F. Abbasalizadeh, S. Fekri Aval, A. A. Khandaghi, et al. (2014). Synthesis and in vitro study of cisplatin-loaded Fe3O4 nanoparticles modified with PLGA-PEG6000 copolymers in treatment of lung cancer. *Journal of Microencapsulation.* **31** (8), 815–823.
40. E. Akbari, H. Mousazadeh, Z. Sabet, T. Fattahi, A. Dehnad, A. Akbarzadeh, et al. (2021). Dual drug delivery of trapoxin A and methotrexate from biocompatible PLGA-PEG polymeric nanoparticles enhanced antitumor activity in breast cancer cell line. *Journal of Drug Delivery Science and Technology.* **61**, 102294.
41. H. Mousazadeh, Y. Pilehvar-Soltanahmadi, M. Dadashpour, and N. Zarghami (2020). Cyclodextrin based natural nanostructured carbohydrate polymers as effective non-viral siRNA delivery systems for cancer gene therapy. *Journal of Controlled Release.* **330**, 1046–1070.
42. S. Amirsaadat, D. Jafari-Gharabaghlou, S. Alijani, H. Mousazadeh, M. Dadashpour, and N. Zarghami (2021). Metformin and Silibinin co-loaded PLGA-PEG nanoparticles for effective

combination therapy against human breast cancer cells. *Journal of Drug Delivery Science and Technology.* **61**, 102107.
43. S. Oh, E. Xiaofei, D. Ni, S. D. Pirooz, J.-Y. Lee, D. Lee, et al. (2011). Downregulation of autophagy by Bcl-2 promotes MCF7 breast cancer cell growth independent of its inhibition of apoptosis. *Cell Death & Differentiation.* **18** (3), 452–464.
44. E. A. Musgrove, C. E. Caldon, J. Barraclough, A. Stone, and R. L. Sutherland (2011). Cyclin D as a therapeutic target in cancer. *Nature Reviews Cancer.* **11** (8), 558–572.